Structural studies of Fe/Pd magnetic multilayers by x-ray diffraction

Y. S. Gu,* W. P. Chai, Z. H. Mai, and J. G. Zhao
Institute of Physics, Chinese Academy of Sciences, P.O. Box 603, Beijing 100080, People's Republic of China

M. Li and L. M. Mei
Department of Physics, Shandong University, Jinan, Shandong 250100, People's Republic of China

C. Dong, F. Wu, and H. Chen
National Laboratory for Superconductivity, Institute of Physics, Chinese Academy of Sciences, P.O. Box 603, Beijing 100080, People's Republic of China

(Received 8 December 1993; revised manuscript received 28 February 1994)

Magnetic multilayers [Fe(20 Å)Pd(t_{Pd})]$_n$ grown by electron-beam evaporation were studied by x-ray small-angle reflection and high-angle diffraction. Structural parameters such as the superlattice periods, the interfacial roughness, the interplanar distances, and the grain sizes were obtained. The experimentally measured superlattrice periods deviated from the nominal ones by a considerable amount. We found that the density of the multilayers had changed abruptly with a Pd layer thickness increase as revealed by the changes of the critical angles and superlattice periods around $t_{Pd}=30$ Å. We also found that the crystal structure of the Fe layer changed from bcc to fcc when the Pd layer thickness $t_{Pd} \geq 36$ Å. Comparison of the saturated magnetization σ_s and the structural perfection showed that the magnetic properties of the Fe/Pd multilayer are strongly structure dependent.

I. INTRODUCTION

Ultrathin magnetic superlattices and multilayers with alternate layers of magnetic and nonmagnetic metals have profound potential in applications and are interesting for the understanding of the fundamental principles involved.[1,2] Since the observation of the giant magnetoresistance (GMR) effect in Fe/Cr multilayers by Baibich *et al.*,[3] great advances have been made in understanding the subject. It is widely accepted that GMR comes from spin-dependent electron scattering by both the interfaces and impurities in the bulk of antiferromagnetically arranged multilayers,[4] which often result from the exchange coupling of the magnetic layers through the nonmagnetic layers. The structure of the multilayer, such as the period, the interfacial roughness, and the crystallinity of each layer, can affect the electric and magnetic properties of the multilayer by changing the magnetic arrangement of the adjacent magnetic layers, the spin dependence, and the strength of electron scattering both at the interfaces and in the bulk. Therefore structural characterization of the multilayers is of great significance in the whole course of research.[5,6]

GMR effects have been observed in many systems. The well-known systems are Fe/Cr and Co/Cu multilayers. For the Fe/Pd multilayer, however, no GMR effect has been observed. Instead, polarization of the Pd layers was discovered and the saturated magnetization was measured experimentally.[7] It is proposed that the polarization of the Pd layers destroys the antiferromagnetic (AF) arrangement of the Fe layers and lead to the disappearance of the giant magnetoresistance. Therefore it is interesting to know how the polarization of the Pd layer destroyed the AF arrangement and to what extent it can affect GMR in other systems.

Since the physical properties of magnetic multilayers are closely related to their structure, structural characterization is of great importance. In normal circumstances, bulk Fe has a body-centered-cubic (bcc) structure with lattice constant $a=2.8655$ Å and Pd has a face-centered-cubic (fcc) structure with lattice constant $a=3.8908$ Å. According to Boufelfel, Emrick, and Falco,[8] Fe/Pd multilayers are grown in such a way that the densest packed planes Fe(110) and Pd(111) are parallel to the surfaces of the multilayers. The lattice mismatch is 4% along the Fe[001] and Pd[01$\bar{1}$] directions and 17% along the Fe[1$\bar{1}$0] and Pd[2$\bar{1}\bar{1}$] directions. Because of the large lattice constants and symmetry mismatches between these two elements, careful characterization of the structure is required. Boufelfel, Emrick, and Falco[8] made structural characterizations on a series of dc-sputtered Fe/Pd multilayers. They used Rutherford backscattering to obtain the chemical composition, standard θ-2θ x-ray diffraction to determine the coherence length, and a Debye-Scherrer camera to find the crystal orientation. Obi *et al.*[9] used a step model to simulate the high-angle x-ray diffraction data and obtained the interplanar distances of a series of rf-sputtered Fe/Pd multilayers with different Fe layer thicknesses. In this paper, a series of Fe/Pd multilayers with varying Pd layer thickness was investigated by both x-ray small-angle reflection and high-angle diffraction, to obtain the superlattice periods, the interplanar distances, the interfacial roughness, the grain sizes, and the structural perfection, etc.

TABLE I. The experimental results of the high-angle x-ray diffraction. For Fe/Pd multilayers with t_{Pd}-thick Pd layer, the period Λ and interplanar distances d_{Pd} and d_{Fe} are obtained from computer simulation of the superlattice peaks.

Sample	1	2	3	4	5	6	7	8	9
t_{Pd} (Å)	16	18	24	28	30	32	36	50	60
θ_1 (deg)	39.90	40.23	40.18	39.82	39.93	40.20	40.15	39.97	39.86
θ_2 (deg)	42.13	42.28	42.04	41.76	41.68	41.58	41.53	41.27	41.07
θ_3 (deg)	44.71	44.37	43.81	43.75	43.71	43.07	43.04	42.71	42.29
I_1 (counts)	48	50	200	245	249	113	97	474	740
I_2 (counts)	100	69	175	295	211	46	61	382	678
I_3 (counts)	13	26	60	40	35	16	27	75	105
Λ (Å)	42.91	44.85	49.30	47.50	51.85	64.97	62.80	65.40	70.11
C_0 (arb. units)	0.051	0.032	0.093	0.102	0.070	0.024	0.025	0.104	0.140
d_{Pd} (Å)	2.168	2.200	2.228	2.224	2.235	2.237	2.240	2.240	2.242
d_{Fe} (Å)	2.027	2.027	2.035	2.039	2.033	2.033	2.078	2.100	2.112

II. EXPERIMENTAL

Fe/Pd multilayers were prepared by electron-beam evaporation. The chamber was initially evacuated to 1×10^{-7} Torr and was at 5×10^{-7} Torr during evaporation. The starting materials for evaporation were Fe (purity 99.95%) and Pd (purity 99.99%). The substrates were 0.1-mm-thick glass plates and were kept at room temperature during evaporation. The deposition rates were about 0.6–0.8 Å/s for Fe and 1.0 Å/s for Pd. Layer thickness was monitored by a quartz crystal oscillator (IL400). A series of multilayer samples was prepared with 25 periods of Pd layers with different thicknesses and 20-Å-thick Fe layers. The nominal parameters of the samples are shown in Table I.

The structural characterization of the samples was carried out by both high-angle and small-angle x-ray measurements. It was done on a Rigaku diffractometer with an 18-kW rotating-anode x-ray generator using a Cu target. Focusing geometry was used in high-angle x-ray diffraction in order to obtain a high intensity. Since high resolution was required for small-angle x-ray reflection, narrow slits and a Si(111) monochromator were used. Procedures were taken to ensure the proper alignment of the orientation and the position of the samples.

To study the magnetic properties of the multilayers, the saturated magnetization σ_s per unit Fe volume was measured by a superconducting quantum interference device (SQUID) at the temperature of 5 K.

III. THEORETICAL CALCULATIONS

The angular position of a superlattice peak is determined by Bragg's law for a superlattice,

$$q_n'=2\pi n/\Lambda\ , \tag{1}$$

where $q_n'=(4\pi/\lambda)\sin\theta_n'$ is the wave-vector transfer in a multilayer, $\Lambda=t_{Fe}+t_{Pd}$ the period of the multilayer, and n the order of the superlattice peak. In the small-angle region, since the angle is comparable to the critical angle θ_c, the refraction of x rays in a multilayer has to be taken into account.[10] Since the critical angle of a multilayer θ_c is related to its average electron density by

$$\theta_c=\sqrt{\rho_e r_e \lambda^2/\pi}\ , \tag{2}$$

where ρ_e is the average electron density, r_e the classical electron radius, and λ the x-ray wavelength, we have

$$q_n^2=q_n'^2+q_c^2\ , \tag{3}$$

where $q_n=(4\pi/\lambda)\sin\theta_n$ is the wave-vector transfer of the nth superlattice peak in air, and $q_c=(4\pi/\lambda)\sin\theta_c$ is the critical wave-vector transfer. Two peaks are enough to determine both the period Λ and critical wave-vector transfer q_c of a multilayer. For the nth and mth peaks, from Eqs. (1) and (3), we have

$$q_c=\left[\frac{m^2q_n^2-n^2q_m^2}{m^2-n^2}\right]^{1/2}\ , \tag{4}$$

$$\Lambda=\frac{2n\pi}{\sqrt{q_n^2-q_c^2}}\ . \tag{5}$$

To analyze the high-angle x-ray diffraction intensities of a multilayer, based on the kinematic diffraction theory,[11,12] we have

$$I(\theta)=CP(\theta)L(\theta)G(\theta)|F(\theta)|^2\ ,$$

where $P(\theta)=1+\cos^2(2\theta)/2$ is the polarization factor, $L(\theta)=1/\sin(2\theta)$ the Lorentz factor, $G(\theta)=1/\sin(\theta)$ the geometry factor, C a constant, and $F(\theta)$ the x-ray structure factor. The x-ray diffraction intensity for a perfect Fe/Pd multilayer becomes

$$I(\theta)=CP(\theta)L(\theta)G(\theta)\left[\frac{\sin(N\Lambda q/2)}{\sin(\Lambda q/2)}\right]^2\left\{\left[f_{Pd}\sigma_{Pd}\frac{\sin(n_{Pd}d_{Pd}q/2)}{\sin(d_{Pd}q/2)}\right]^2+\left[f_{Fe}\sigma_{Fe}\frac{\sin(n_{Fe}d_{Fe}q/2)}{\sin(d_{Fe}q/2)}\right]^2 +2f_{Pd}f_{Fe}\sigma_{Pd}\sigma_{Fe}\frac{\sin(n_{Pd}d_{Pd}q/2)}{\sin(d_{Pd}q/2)}\frac{\sin(n_{Fe}d_{Fe}q/2)}{\sin(d_{Fe}q/2)}\cos(\Lambda q/2)\right\}\ , \tag{6}$$

where $q=(4\pi/\lambda)\sin\theta$ is the wave-vector transfer, f_{Pd} and f_{Fe} are the atomic scattering factors of x rays, σ_{Pd} and σ_{Fe} the atomic densities in a monolayer, n_{Pd} and n_{Fe} the numbers of monolayers in each period, d_{Pd} and d_{Fe} the interplanar distances, the subscripts Pd and Fe denote the two elements, palladium and iron, respectively, N is the number of periods in a multilayer, and Λ the superlattice period.

In fact, a real Fe/Pd multilayer sample prepared by electron-beam evaporation consists of a large number of grains with different sizes and structural parameters. The total x-ray diffraction intensity of the sample is the summation of the x-ray diffraction intensities of each grain,

$$I_{\mathrm{total}}(\theta)=\sum_i C_i I_i(\theta) , \tag{7}$$

where C_i is the number of grains with the ith set of structural parameters, and $I_i(\theta)$ is the x-ray diffraction intensity of a grain with that set of structural parameters as calculated by Eq. (6). The summation is over all the possible sets of structural parameters.

Small-angle x-ray reflectivity should be calculated by the dynamical theory of x-ray diffraction. The recursion formula of Parratt[13] often used to calculate the x-ray reflectivity of multilayers is a good example. It is the case especially when the superlattice has high crystallinity, long period, large number of periods, and sharp interfaces so that the reflectivity is close to unity. If a multilayer has only a moderate number of periods so that the reflectivity at a superlattice peak is far less than 1, we may apply a modified kinematic theory to calculate the peak intensity. The reflection coefficient of the nth superlattice peak is given by

$$r_n=r_t+Nr[\exp(iqt_{\mathrm{Fe}})-1]+r_b ,$$

where r_t and r_b are the reflection coefficients at the top and the bottom faces of the multilayer, respectively, r is that of the interfaces between Fe and Pd layers, and t_{Fe} is the thickness of the Fe layers. Since $N\gg 1$, r_t and r_b can be neglected. The reflectivity becomes[10]

$$R_n=N^2\left[\frac{\Delta q_c^2}{2q_n'^2}\right]^2\sin^2(n\pi t_{\mathrm{Fe}}/\Lambda)\exp(-q_n'^2\sigma^2) , \tag{8}$$

where Δq_c^2 is the difference of q_c^2 between two layers and σ the interfacial roughness. The ratio of the intensity of the nth and mth superlattice peaks can eliminate some common proportional constants. From Eq. (1), we have

$$\frac{R_n}{R_m}=\left[\frac{m}{n}\right]^4\frac{\sin^2(n\pi t_{\mathrm{Fe}}/\Lambda)}{\sin^2(m\pi t_{\mathrm{Fe}}/\Lambda)}\times\exp[-4\pi^2(n^2-m^2)\sigma^2/\Lambda^2] .$$

Therefore the interfacial roughness is

$$\sigma=\frac{\Lambda}{2\pi\sqrt{n^2-m^2}}\left[\ln\left[\frac{R_m}{R_n}\right]-4\ln\left[\frac{n}{m}\right]-2\ln\left|\frac{\sin(m\pi t_{\mathrm{Fe}}/\Lambda)}{\sin(n\pi t_{\mathrm{Fe}}/\Lambda)}\right|\right]^{1/2} . \tag{9}$$

IV. RESULTS AND DISCUSSIONS

The experimental results of high-angle x-ray diffraction are shown in Fig. 1. We can see two or three main superlattice peaks on each curve. The angle positions (θ_n) and the intensities (I_n) of the superlattice peaks are shown in Table I. After a small decrease for sample 2, the intensity of the superlattice peaks increases with Pd layer thickness until it reaches a maximum for sample 4. Then it decreases with Pd layer thickness until it reaches a minimum for sample 6. The intensities increase again with Pd layer thickness. The interval between the superlattice peaks becomes smaller as the Pd layer thickness t_{Pd} increases. The widths of the superlattice peaks also change with Pd layer thickness in such a way that high peaks have narrow widths and low ones have broad widths.

High-angle x-ray diffraction intensity is related to the structural parameters of the samples by Eqs. (6) and (7). Therefore computer simulation of the intensity of the superlattice peaks yields structural parameters of the samples, such as the superlattice periods Λ, the interplanar distances d_{Pd} and d_{Fe}, the average grain sizes, and the proportionality constant C_i. Computer simulation of the x-ray diffraction intensities was done as follows. First, the intensities and angular positions of the main superlattice peaks are used to determine roughly the structural parameters of the majority of the grains. Then the profiles of these peaks are simulated by including grains with different sizes. The average grain sizes can be obtained. Finally, the shoulders on the main peaks and the small peaks between them are fitted by including grain with different superlattice periods and then interplanar distances. The structural parameters are refined in the process of simulation of the experimental x-ray diffraction data. Figure 2 shows an example of computer simulation of the high-angle x-ray diffraction curve for sample 4. One can see the good match of the computer simulation to the experimental data. The structural parameters obtained for the majority of grains are

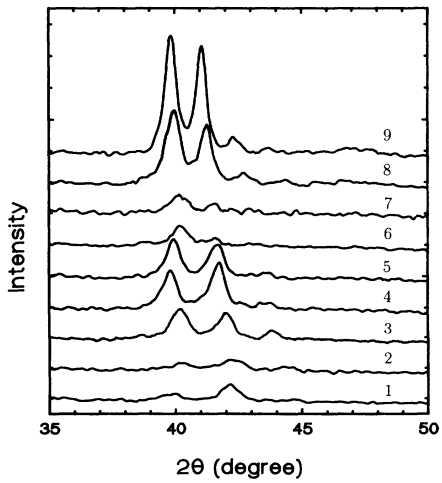

FIG. 1. High-angle x-ray diffraction curves of the Fe/Pd multilayers.

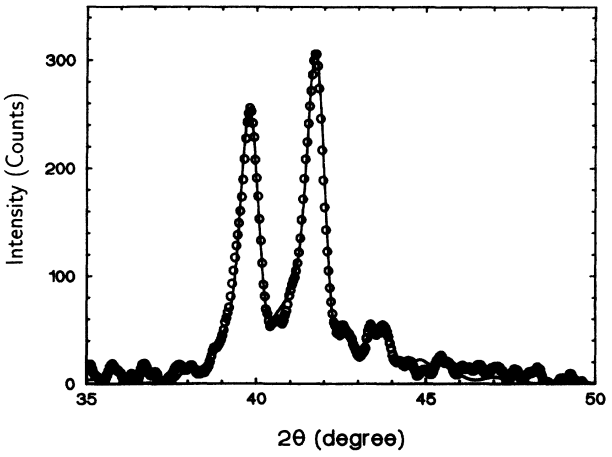

FIG. 2. Computer simulation (solid line) of high-angle x-ray diffraction data (circles) of sample 4.

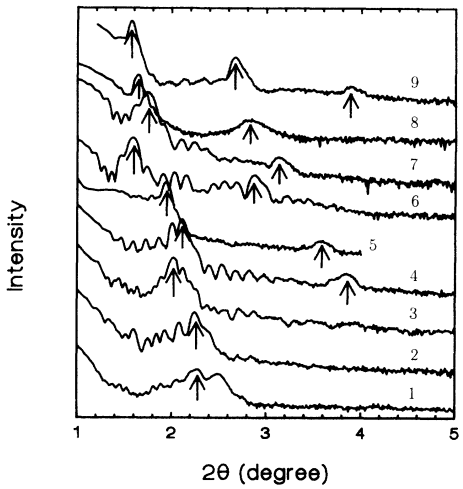

FIG. 3. Small-angle x-ray reflectivity curves of the Fe/Pd multilayers.

$\Lambda=47.50$ Å, $d_{Fe}=2.039$ Å, $d_{Pd}=2.224$ Å, and the average grain size $D=124$ Å. At the same time, there is a small fraction of grains with superlattice periods $\Lambda=46.50$ Å and 48.20 Å. Some grains even have interplanar distances $d_{Pd}=2.17$ Å. From the above simulation, one can see a picture of the real structure of the Fe/Pd multilayers. The results of the computer simulation for the main peaks of all the samples are listed in Table I, and will be discussed in the following subsections.

The small-angle x-ray reflectivity curves of the Fe/Pd multilayers are shown in Fig. 3. We can see the superlattice peaks (indicated by arrows) as well as Kiessig fringes on each curve. Samples with $t_{Pd} \geq 28$ Å have two or three superlattice peaks while the others have only one superlattice peak with low intensity. The angular position of the superlattice peaks decreases with increasing Pd layer thickness with the exception of samples 4 and 7. The angular positions and intensities of the superlattice peaks are listed in Table II.

The critical angle θ_c can be derived by Eq. (4) for the samples with two or more superlattice peaks on the x-ray reflectivity curves, and it is calculated by Eq. (2) for samples with only one superlattice peak. The superlattice periods Λ of the samples are calculated from the angular positions of the superlattice peaks by Eq. (5). All the experimental results are listed in Table II, and will be discussed in the following subsections.

A. Structural specifications

The period of the multilayers is an important structural parameter which can affect the magnetic properties of the samples. Therefore, accurate measurement is required. The superlattice periods obtained from small- and high-angle diffraction are shown in both Table I and Table II. It is clear that these two results are in good agreement with each other. However, there is a large difference between them and the nominal periods $[\Lambda_0=(20\ \text{Å})+t_{Pd}]$ obtained by a quartz crystal oscillator during growth. Since the oscillator is sensitive only to the mass density per unit area, it does not directly determine layer thickness. Since the samples studied in this paper consist of ultrathin layers with large lattice mismatches, the layers are presumably strongly distorted. The calibration errors as well as the fluctuation of the density of the distorted layers together can cause large measurement errors in the layer thickness. Therefore it is very important to determine the superlattice periods experimentally in order to obtain magnetic properties correctly.

TABLE II. Experimental results of small-angle x-ray reflection. The superlattice periods Λ, the critical angle θ_c, and the interfacial roughness σ of Fe/Pd multilayers are obtained from the angular positions (θ_n) and intensities (I_n) of the superlattice peaks. The data in parenthesis are theoretical.

Sample	1	2	3	4	5	6	7	8	9
θ_1 (deg)	2.269	2.250	2.019	2.112	1.940	1.589	1.749	1.648	1.579
θ_2 (deg)				3.843	3.580	2.878	3.131	2.840	2.672
I_1 (counts)	2725	25 100	145 000	144 000	106 000	217 000	424 200	31 540	192 400
I_2 (counts)				185	80	2575	172	132	2690
Λ (Å)	42.38	42.81	48.84	47.63	50.62	63.72	58.88	66.11	70.93
θ_c (deg)	(0.45)	(0.45)	(0.45)	0.506	0.432	0.389	0.450	0.483	0.486
σ (Å)				7.01	8.65	5.78	11.80	10.77	9.65

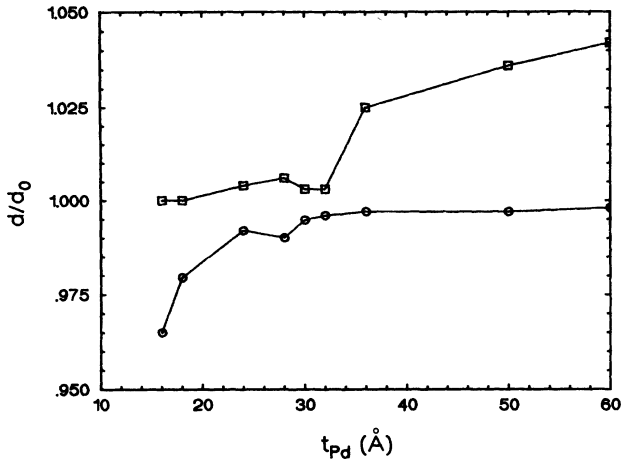

FIG. 4. Ratio of d/d_0 as a function of t_{Pd} for Pd layer (circles) and Fe layer (squares).

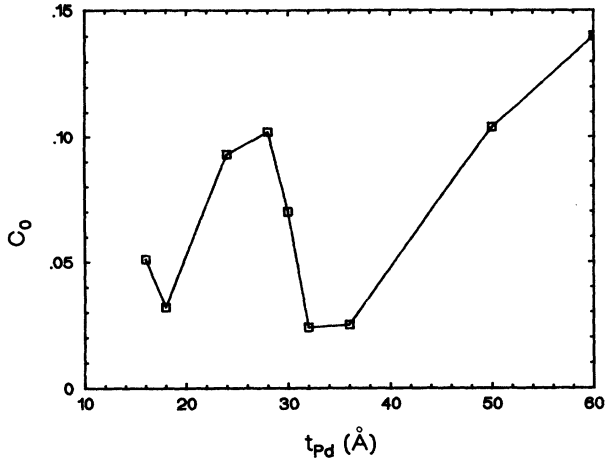

FIG. 5. Constant C_0 in Eq. (7) as a function of t_{Pd}.

The interplanar distances of the Pd and Fe layers, d_{Pd} and d_{Fe} are the distances between the monolayers parallel to the surface of the samples. Presumably, these values are close to the interplanar distances of the fcc Pd(111) and the bcc Fe(110) planes. The experimental results obtained by computer simulations of the high-angle x-ray diffraction intensities are listed in Table I. Figure 4 shows the ratio of the experimental interplanar distances to those of the bulk as a function of Pd layer thickness. One can see that the interplanar distances d_{Pd} are compressed and d_{Fe} are expanded in the multilayers. This contradicts the results reported by Obi *et al.*,[8] which show compressed Fe layers and expanded Pd layers. As the Pd layer thickness t_{Pd} increases, the interplanar distance of the Pd layers d_{Pd} increases quickly at first and gradually approaches the value of the interplanar distance of fcc Pd(111) planes. At the same time, the interplanar distance of the layers d_{Fe} increases from the interplanar distance value of the bcc Fe(110) planes ($d=2.027$ Å) until $t_{Pd}=28$ Å. After decreasing slightly at $t_{Pd}=30$ and 32 Å, it increases abruptly at $t_{Pd}=36$ Å and gradually approaches the value of the interplanar distance of the fcc Fe(111) planes ($d=2.106$ Å).

The interfacial roughness of the multilayers can be obtained from the relative intensity of the superlattice peaks in the x-ray reflectivity curves by Eq. (9). As shown in Table II, the interfacial roughness is about 6–12 Å and tends to increase with the period of the sample. The interfacial roughness is much smaller than the layer thickness, so the Fe and Pd layers of the multilayers are separated very well. The multilayer is periodic in composition.

B. Structural perfection

The structural perfection of the multilayers can be revealed by x-ray diffraction experiments in both small- and high-angle regions. The observation of high-angle superlattice peaks is an indication that the samples have good periodicity as well as structural coherence, since the high-angle superlattice peaks disappear for incoherent multilayers according to Fullerton and Schuller.[14] The intensities of the superlattice peaks are indications of the structural perfection and are described by the proportionality constants C_i as defined in Eq. (7). The constant for the majority of grains C_0 as a function of t_{Pd} shows the change of structural perfection with Pd layer thickness. As shown in Fig. 5, as the Pd layer thickness increases, after a small decrease at $t_{Pd}=18$ Å, the constant C_0 increases and reaches a maximum at $t_{Pd}=30$ Å, then decreases until it reaches a minimum at $t_{Pd}=36$ Å, and then it increases again with the increase of Pd layer thickness. This suggests that the structural perfection is poor for the samples with thin Pd layers, and improves as the Pd layer thickness increases until it reaches a maximum at $t_{Pd}=28$ Å. Then it degrades as t_{Pd} increases further until $t_{Pd}=32$ Å. After that, the structural perfection improves again as the Pd layer thickness increases.

The small-angle x-ray reflectivity is sensitive to the modulation of the chemical composition of the multilayers. The intensity of the superlattice peaks in the reflectivity curves shows the goodness of the composition modulation of the samples. From Table II, one can see that the intensity of the first superlattice peaks is rather low for the samples with $t_{Pd}\leq 20$ Å, and becomes extremely high for samples with $t_{Pd}\geq 24$ Å. This means that the composition modulation of the samples is good for samples with thick layers and long period.

The change of grain size (D) with t_{Pd} shows the change of the structural coherence with the period of the multilayers. The average grain sizes are obtained from computer simulation of the profile of the superlattice peaks. From Fig. 6, one can see that the average grain size is about 100 Å, i.e., about 2–3 periods of the multilayers. After a decrease at $t_{Pd}=18$ Å, the grain size increases with increase of t_{Pd} and reaches a maximum at $t_{Pd}=30$ Å, then decreases again until $t_{Pd}=36$ Å, and increases again. This suggests that the coherence of the multilayer is getting better at first until it reaches a maximum at $t_{Pd}=30$ Å, and then it gets worse as t_{Pd} increases until it reaches a minimum at $t_{Pd}=36$ Å. It then gets better for

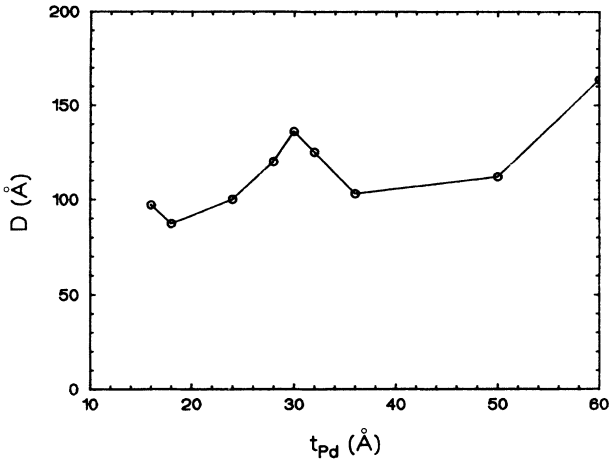

FIG. 6. Average grain size D as a function of t_{Pd}.

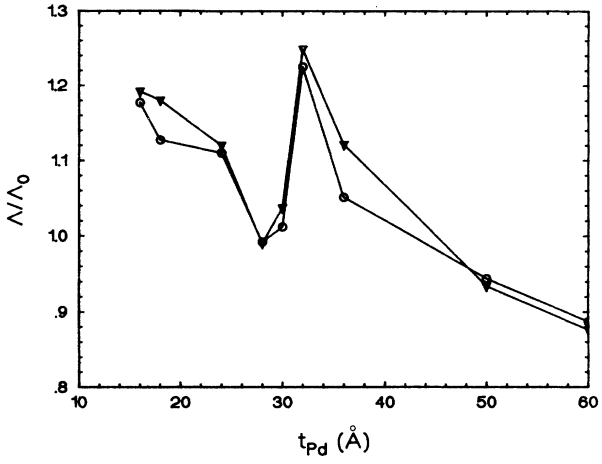

FIG. 7. Ratio of Λ/Λ_0 as a function of t_{Pd}, from high-angle diffraction (triangles) and small-angle reflection (circles).

samples with $t_{Pd} \geq 36$ Å.

From the above experimental results, the Fe/Pd multilayers with thin Pd layers ($t_{Pd} \leq 20$ Å) have poor structural perfection. This might be caused by the poor crystallinity of the thin Pd layers. As the Pd layer thickness t_{Pd} increases, the structural perfection gets better. This is due to the improved crystallinity of the Pd layers. When $t_{Pd} \geq 30$ Å, the structural perfection of the samples degrades as t_{Pd} increases. This is caused by the large lattice mismatch between the two component layers. As the layers become thick, they tend to form structures similar to that of the bulk. This increases the strains between the layers and leads to the reduction of the coherence length and poor interfaces. When the Pd layer thickness $t_{Pd} \geq 36$ Å, the structural perfection of the multilayers gets better again. This is caused by the structural transition of the Fe layers from bcc to fcc, since the fcc Fe(111) planes match the fcc Pd(111) planes much better than the bcc Fe(110) planes do. This is supported by the change of interplanar distance of the Fe monolayers from that of the bcc Fe(110) planes ($d=2.027$ Å) to that of the fcc Fe(111) planes ($d=2.106$ Å) with a jump at $t_{Pd}=36$ Å, as shown in Table I and Fig. 4. The Fe layer is forced to transform from its normal bcc structure into its fcc structure which matches well with the fcc Pd layer (6.7% lattice mismatch) by the strong lattice force of the thick Pd layer ($t_{Pd} \geq 36$ Å).

C. Abrupt changes of average density

The ratio of the experimental superlattice periods to the nominal ones Λ/Λ_0 for small- and high-angle x-ray diffraction as a function of the Pd layer thickness is shown in Fig. 7. We can see an abrupt change of the ratio at $t_{Pd}=28$ and 32 Å. Meanwhile, as shown in Table II, the critical angle θ_c changes abruptly at $t_{Pd}=28$ and 32 Å, corresponding to the changes of the superlattice periods. Since the average density of the multilayer is related to its critical angle by Eq. (2), we can conclude that the abrupt changes of Λ/Λ_0 and θ_c are caused by the change of the average density of the multilayers. Since $\rho \propto \theta_c^2$, and $\Lambda \propto \rho^{-1/3}$, modification of the period thickness by $\Lambda_m = \Lambda(\theta_c/\theta_{c0})^{2/3}$ should eliminate the effect of density change on the period Λ. The results of Λ_m/Λ_0 are plotted in Fig. 8 for both small- and high-angle experiments. We can see that the modified superlattice period is more closely related to the nominal parameters given by a quartz crystal oscillator. The abruptness of the change of the ratio of the superlattice periods is reduced. Therefore the change of the average density of the multilayers causes the abrupt change of the ratio of the superlattice periods.

D. Saturated magnetization

The saturated magnetization per unit Fe volume σ_s of the Fe/Pd multilayers at $T=5$ K as a function of the Pd layer thickness is shown in Fig. 9. The results are modified by the experimental superlattice periods. One

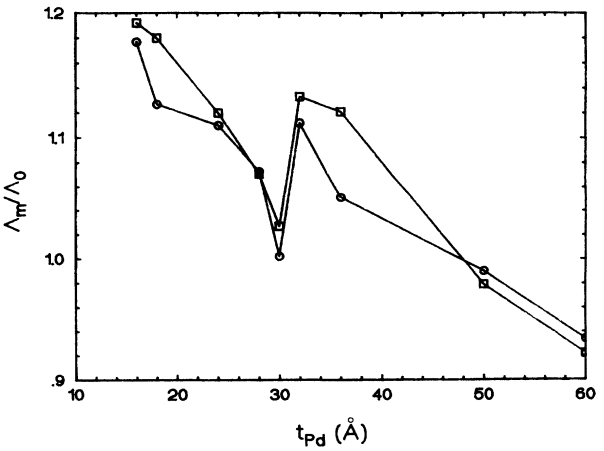

FIG. 8. Ratio of Λ_m/Λ_0 as a function of t_{Pd}, from high-angle diffraction (squares) and small-angle reflection (circles).

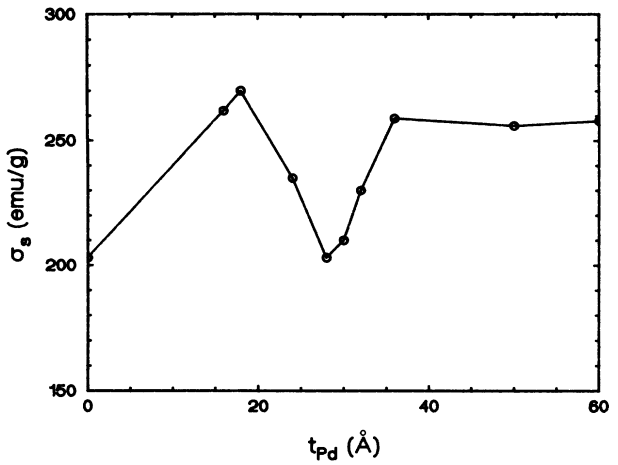

FIG. 9. Saturated magnetization per unit Fe volume σ_s as a function of the thickness of the Pd layers t_{Pd}.

can see that the magnetization increases with increasing Pd layer thickness until it reaches a maximum at about 18 Å, then decreases and reaches a minimum at about 28 Å. It increases again until it reaches a saturated value for $t_{Pd} \geq 36$ Å. The saturated magnetization σ_s is larger than that of pure iron. The increase of σ_s might be caused by the polarization of the Pd layers.[7] The maximum of σ_s at $t_{Pd} = 18$ Å coincides with the drop of the intensity constant C_0 and coherence length of the sample. The minimum at $t_{Pd} \approx 30$ Å also coincides with the maximum of the intensity constant C_0 and coherence length at that Pd layer thickness. Therefore the saturated magnetization σ_s is related to the structural perfection of the multilayer. Structure is an important factor to consider in the study of the magnetic properties of the samples.

V. CONCLUSIONS

We have studied a series of Fe/Pd multilayers grown by electron-beam evaporation by x-ray small-angle reflection and high-angle diffraction. The superlattice periods, the interplanar distances, the coherence length, the interfacial roughness, and the critical angles are obtained. The superlattice periods deviate by a large amount from the nominal ones. The interplanar distances of the Pd layer d_{Pd} are compressed from that of bulk fcc Pd(111) planes and decrease as the Pd layer thickness decreases, while the interplanar distances of Fe layers d_{Fe} are expanded from that of bulk bcc Fe(110) planes and increase with increases of Pd layer thickness. There is a jump at about $t_{Pd} = 36$ Å to that of the bulk fcc Fe(111) planes. The interfacial roughness is 6–12 Å. The abrupt change of the superlattice period and critical angle at about $t_{Pd} = 30$ Å indicates changes of the density of the multilayers. From the experimental results, we found that the crystal structure of the Fe layers changes from its normal bcc structure to its fcc structure, which matches with the Pd fcc structure very well, at $t_{Pd} \approx 36$ Å. The saturated magnetization σ_s of the multilayer is related to the structural perfection of the sample. A high and stable value of σ_s for samples with $t_{Pd} \geq 36$ Å shows that the fcc Fe layers have higher saturated magnetization than the bcc Fe layers. This suggest that the structure is an important factor in the study of the magnetic properties of the multilayers.

ACKNOWLEDGMENTS

This work benefited from many helpful discussions with M. L. Yan, who introduced to us this exciting field of study. Professor D. S. Dai from the Department of Physics, Beijing University helped us a lot during sample preparation.

*Author to whom all correspondence should be addressed.

[1]L. M. Falicov, Phys. Today **45**(10), 46 (1992).
[2]R. L. White, IEEE Trans. Magn. **28**, 2482 (1992).
[3]M. N. Baibich, J. M. Broto, A. Fert, F. Nguyen Van Dan, F. Petroff, P. Eitenne, G. Creuzet, A. Friederich, and J. Chazelas, Phys. Rev. Lett. **61**, 2472 (1988).
[4]P. M. Levy, K. Ounadjela, S. Zhang, Y. Wang, C. B. Sommers, and A. Fert, J. Appl. Phys. **67**, 5914 (1990).
[5]E. E. Fullerton, D. M. Kelley, J. Guimpel, I. K. Schuller, and Y. Bruynseraede, Phys. Rev. Lett. **68**, 859 (1992).
[6]T. Dei, R. Nakatani, and Y. Sugita, Jpn. J. Appl. Phys. **32**, 1097 (1993).
[7]H. R. Zhai, H. Wang, M. Lu, H. Y. Zhang, S. M. Zhou, Y. H. Liu, L. Zhang, and L. M. Mei, J. Magn. Magn. Mater. **104-107**, 1825 (1992).
[8]A. Boufelfel, R. M. Emrick, and C. M. Falco, Phys. Rev. B **43**, 13 152 (1991).
[9]Y. Obi, Y. Kawano, Y. Tange, and H. Fujimori, J. Magn. Magn. Mater. **93**, 587 (1991).
[10]J. Als-Nielsen, in *Structure and Dynamics of Surfaces,* edited by W. Schommers and P. von Blackenhagen (Springer-Verlag, Berlin, 1987), Vol. II, p. 181.
[11]G. Gladyszewski, Thin Solid Films **204**, 473 (1991).
[12]T. Shinjo and T. Takada, *Metallic Superlattices—Artificially Structured Materials* (Elsevier, Amsterdam, 1987).
[13]L. G. Parratt, Phys. Rev. **95**, 359 (1954).
[14]E. E. Fullerton and I. K. Schuller, Phys. Rev. B **45**, 9292 (1992).